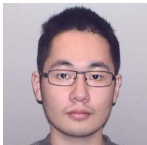


# SD-DP: Sparse Dual of the Density Peaks Algorithm for Cluster Analysis of High-Dimensional Data

November 5, 2018



Dimitris Floros<sup>1</sup>



Tiancheng Liu<sup>2</sup>



Nikos Pitsianis<sup>12</sup>



Xiaobai Sun<sup>2</sup>

<sup>1</sup>Department of Electrical and Computer Engineering, Aristotle University of Thessaloniki

<sup>2</sup>Department of Computer Science, Duke University

The first two authors contributed equally to this work

1. Cluster analysis of high-dimensional data
2. The Density Peaks (DP) and other influential algorithms
3. SD-DP: Sparse Dual of the DP algorithm
4. Experimental evidence
  - Benchmarks
  - Exploratory results

1. **Cluster analysis of high-dimensional data**
2. The Density Peaks (DP) and other influential algorithms
3. SD-DP: Sparse Dual of the DP algorithm
4. Experimental evidence
  - Benchmarks
  - Exploratory results

# Cluster analysis of high-dimensional data

**Premise:** intrinsic heterogeneous group/cluster structures in real-word data of research interest

**Cluster analysis:** uncover cluster structures in data, with noise and uncertainty, with quantified features, governed by certain differentiation criteria

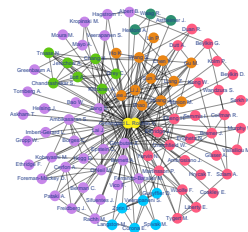
- massive data of many attributes/features
- supervised vs. *un-supervised*

Fundamental to various research studies

Domain-specific analysis	Feature description
Molecular dynamics trajectory patterns [1]	kinetic, spectral measurements
Classification of astronomical events [2]	Gamma ray measurements
Community detection in complex system [3, 4, 5]	link features
Image segmentation/denoising [6, 7]	intensity, patch texture
Content-based image retrieval [8]	semantic content descriptor
Image object recognition [9, 10]	SIFT [11], HOG [12] descriptors
Gene expression pattern analysis [13, 14, 15, 16, 17]	gene-expression matrix
Thematic categorization of documents [18, 19]	word frequency vector
Statistical semantic or sentiment analysis	GloVe [20] word vector
Statistical categorization of musical genres [21]	musical surface features
Consumer profiling/market segmentation [22]	purchase history



Abell 901/902 supercluster [23]



Co-authorship communities [25]



US city lights [26]

$\backslash[-1.5\text{em}]$

Uber & Taxi demand in NYC [24]



1. Cluster analysis of high-dimensional data

**2. The Density Peaks (DP) and other influential algorithms**

3. SD-DP: Sparse Dual of the DP algorithm

4. Experimental evidence

- Benchmarks
- Exploratory results

# DP, other influential algorithms & SD-DP

Algorithms Desirable properties <sup>1</sup>	K-MEANS [27] (1982)	DBSCAN [28] (1996)	OPTICS [29] (1999)	MEAN SHIFT [30] (2002)	GN [3] (2002)	COMBO [5] (2014)	DP [31] (2014)	SD-DP [32] (2018)
No prescription of # clusters		✓	✓	✓	✓	✓	✓	✓
No restriction in cluster shape		✓	✓	✓	✓	✓	✓	✓
Free choice of metrics		✓	✓		✓	✓	✓	✓
Agnostic to distribution		✓	✓	✓			✓	✓
Easy or no tuning	✓				✓	✓		✓
Robust in high-dim. space								✓
Accurate in high-dim. space								✓
Low computation cost								✓

Checkmarks are based on limited benchmarking experiments

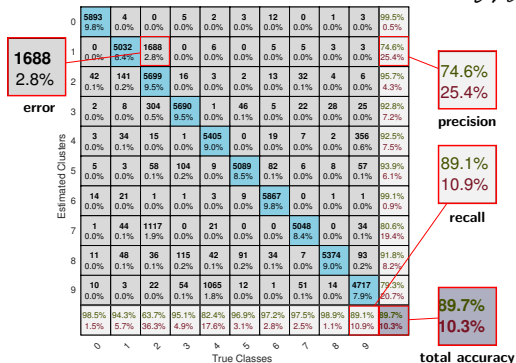
<sup>1</sup> Additional properties include low program complexity, stability and more

# DP vs SD-DP: classification accuracy

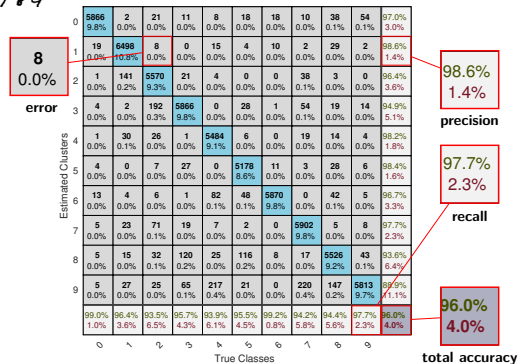
60,000 images of handwritten digits (MNIST dataset) [33]

0 1 2 3 4 5 6 7 8 9  
0 1 2 3 4 5 6 7 8 9  
0 1 2 3 4 5 6 7 8 9  
0 1 2 3 4 5 6 7 8 9  
0 1 2 3 4 5 6 7 8 9

DP (2018) [34]



SD-DP



Intensity feature vector ( $D = 28 \times 28 = 784$ )

Tangent distance

Manual intervention in peak selection and cluster merge

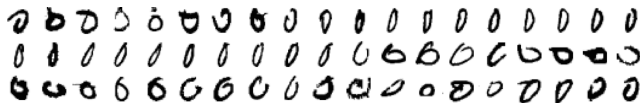
HOG descriptors ( $D = 144$ )

Euclidean distance

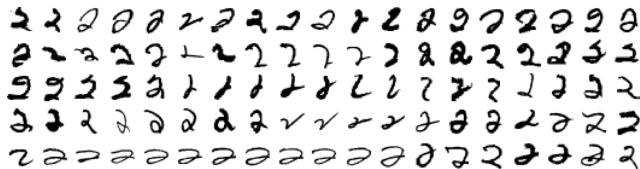
Unsupervised cluster revision

# DP vs SD-DP: classification accuracy

Digit	DP (2018) semi-supervised	SD-DP un-supervised
0	0.99	0.98
1	0.83	0.98
2	0.77	0.95
3	0.94	0.95
4	0.87	0.96
5	0.95	0.97
6	0.98	0.98
7	0.88	0.96
8	0.95	0.94
9	0.84	0.93



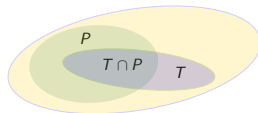
All misclassified digit-0 images by SD-DP



Subset of misclassified digit-2 images by SD-DP

Comparison in Dice similarity coefficients (DSC)  
a.k.a. F1 scores and Sørensen-Dice coefficients  
60,000 images of handwritten digits (MNIST dataset)

$$\text{DSC} = \frac{2TP}{2TP + FP + FN} = \frac{2|T \cap P|}{|T| + |P|}$$



1. Cluster analysis of high-dimensional data
2. The Density Peaks (DP) and other influential algorithms
- 3. SD-DP: Sparse Dual of the DP algorithm**
4. Experimental evidence
  - Benchmarks
  - Exploratory results

# The Density Peaks principle

[Rodriguez and Laio, Science, 2014]

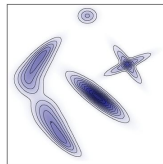
## Principle

*“Cluster centers are characterized by a higher density than their neighbors and by a relatively large distance from points with higher densities”.*

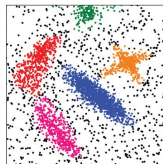
## Local density description

population in neighborhood of specified radius  $r$

$$\rho_i = \begin{cases} |\mathcal{N}_r(x_i)|, & \text{hard cutoff} \\ \sum_j \exp(-d_{ij}^2/r^2), & \text{soft cutoff} \end{cases}$$



Probability distribution from which point distributions are drawn. The regions with lowest intensity correspond to a background uniform probability of 20%.



Point distribution for samples of 4000 points. Points are colored according to the cluster to which they are assigned. Black points belong to the cluster halos.

# Fundamental facts about deep feature space

Deep feature space<sup>1</sup>:  $D > 100$

Fact 1:

$$2^D \gg N$$

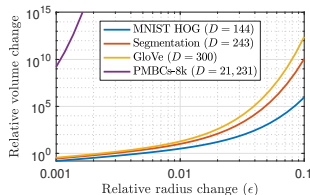
Data are **sparsely, non-uniformly** scattered

Fact 2: With  $D$  fixed, the hyper-ball volume is **highly sensitive** to radius change

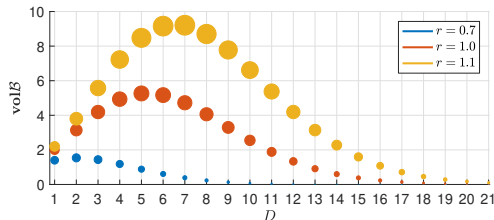
$$\text{vol}\mathcal{B}(r(1+\epsilon))/\text{vol}\mathcal{B}(r) = (1+\epsilon)^D$$

Fact 3: With radius  $r$  fixed, the hyper-ball volume is **vanishing**

$$\text{vol}\mathcal{B}(r) \rightarrow 0 \text{ as } D \rightarrow \infty$$



Fact 2 on specific feature dimensions for 4 particular datasets



Fact 3 on 3 radius values at the low end of dimensions  
Each hyper-ball  $\mathcal{B}$  is depicted by the disk of area  $\text{vol}\mathcal{B}(r)$

<sup>1</sup> Largest database (as of 2018): World Data Center for Climate (WDCC) – 6 petabytes ( $2^{50}$  bytes) of data

# Limitations of DP in deep feature space

By the fundamental Facts about data  
in a deep feature space

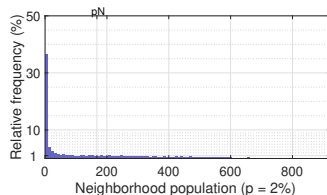
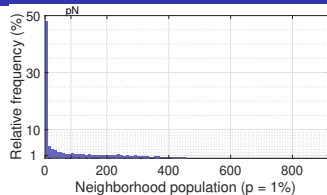
- small radius  $\rightarrow$  many *empty* neighborhoods
- large radius  $\rightarrow$  many *equally crowded* neighborhoods
- adequately discriminative radius values are *elusive*

Rodriguez and Laio suggested a heuristic approach: let radius

$$r = \min_d \left\{ d \mid \sum_i |\mathcal{N}_d(x_i)| \geq p N^2 \right\}$$

with  $p = 1\%$ ,  $2\%$  so that  $\text{avg}(\rho) = p N$

See the histograms to the right



Histograms of neighborhood population, over 50 equispaced bins, with dataset PBMCs-8k of  $N = 8,000$  cells,  $D = 21,321$  genes [35]. The neighbor radius values are determined by the heuristic described on the left with  $p = 1\%$ ,  $2\%$  for the top and bottom histograms, respectively. In each case, the local density at a large portion of data points is close to zero

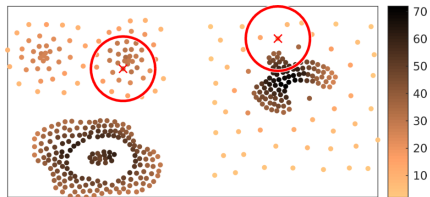


# Duality in local density description: neighborhood radius vs population

## DP $\rho(r)$

#neighbors within distance  $r$

$$\rho_i(r) = \begin{cases} |\mathcal{N}_r(x_i)|, & \text{hard cutoff} \\ \sum_j \exp(-d_{ij}^2/r^2), & \text{soft cutoff} \end{cases}$$



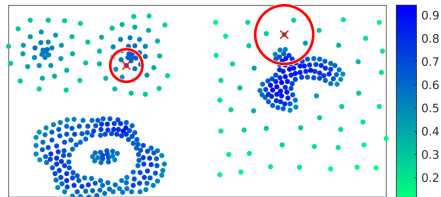
Local density  $\rho$  with  $r = 3.1$

Free parameter  $r$ : real-valued  
elusive, volatile in deep space

## SD-DP $\rho^*(k)$

reciprocal distance to the  $k$ -th nearest neighbor

$$\rho_i^*(k) = 1 / \max_j \{d_{ij} \mid x_j \in \mathcal{N}_k(x_i)\}$$



Dual local density  $\rho^*$  with  $k = 15$

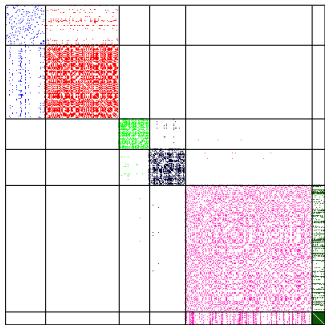
Free parameter  $k$ : discrete  
within grasp, tunable in deep space

# Duality in local density description: neighborhood size vs population

## DP

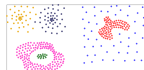
#neighbors within distance  $r$

$$\rho_i = \begin{cases} |\mathcal{N}_r(x_i)|, & \text{hard cutoff} \\ \sum_j \exp(-d_{ij}^2/r^2), & \text{soft cutoff} \end{cases}$$



$\mathbf{G}_r$ : rNN matrix (Boolean values)  
rows/columns ordered by true classes

Labeled Data  
Compound

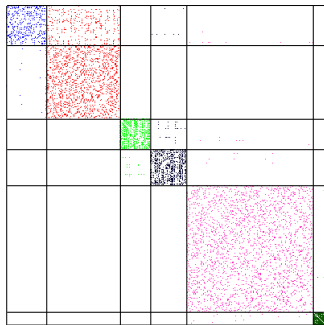


399 points  
6 classes

## SD-DP

reciprocal distance to the  $k$ -th nearest neighbor

$$\rho_i^* = 1 / \max_j \{d_{ij} \mid x_j \in \mathcal{N}_k(x_i)\}$$



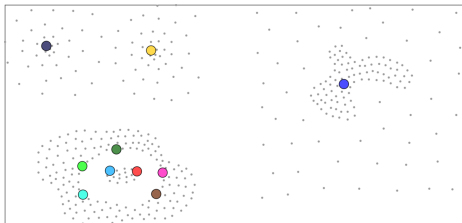
$\mathbf{G}_k$ : kNN matrix (Boolean values)  
rows/columns ordered by true classes

# Density peak location

## DP

Density peaks are located on  $\rho$ - $\delta$  **decision graph**

- chosen heuristically or manually
- $O(N^2)$  for  $\rho$ - $\delta$  graph construction

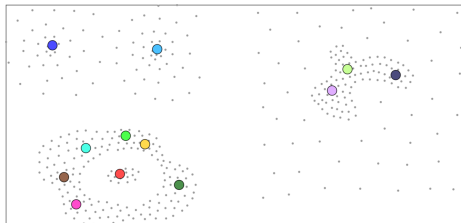


Compound density peaks (color-coded) with  $r = 3.1$

## SD-DP

Density peaks are **local maxima** in density

- determined simultaneously, automatically
- $O(N)$ , each point makes comparisons with  $k$  neighbors



Compound dual density peaks (color-coded) with  $k = 15$

Each peak holds a unique label  
The rest get labels by **ascending** to the peaks

# Ascending rule & $\rho$ - $\delta$ graph

## Ascending rule

Every non-peak point  $i$  connects to its *nearest* point of *higher* density

$$x_i = \arg \min_j \{d_{ij} \mid \rho_j > \rho_i\}, \quad \text{parental node}$$

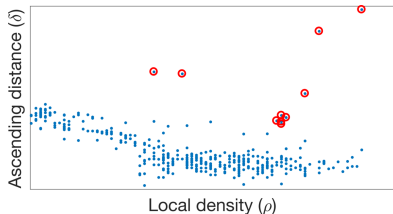
$$\delta_i = \min_j \{d_{ij} \mid \rho_j > \rho_i\}, \quad \text{ascending distance}$$

$O(N^2)$  for  $\rho$ - $\delta$  graph construction

**DP decision graph** in the  $\rho$ - $\delta$  plane

*Mandatory* for peak selection by the heuristic:

“only points of high  $\delta$  and high  $\rho$  are the cluster centers”

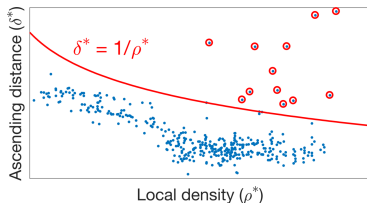


DP decision graph with dataset **Compound** for peak selection  
Red circles annotate density peaks

$O(N)$ , parents located locally on the  $k$ NN graph

**SD-DP ( $\rho^*$ - $\delta^*$ ) graph**

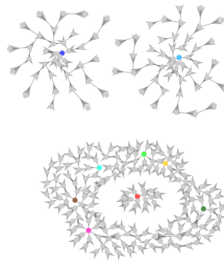
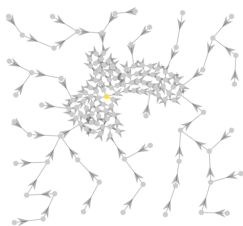
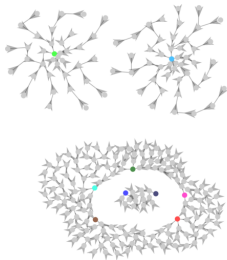
Visualizing the proven properties of autonomous,  
linear-cost separation of local maxima from the rest



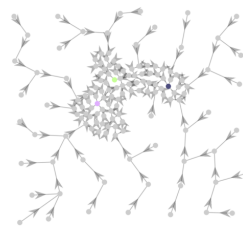
SD-DP visualization graph with dataset **Compound**  
Red circles annotate local maxima

# Label propagation by ascending rule

DP



SD-DP

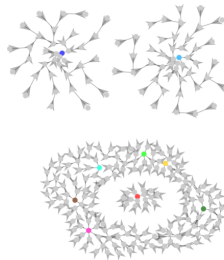


Animation of label propagation with dataset **Compound**

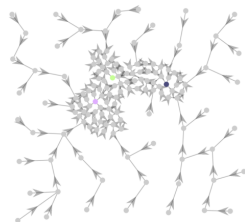
Each peak holds a unique label  
The rest get labels by **ascending** to the peaks

# Label propagation by ascending rule

DP



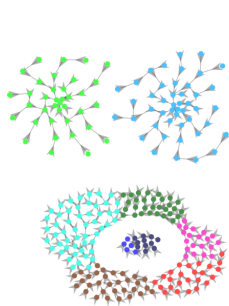
SD-DP



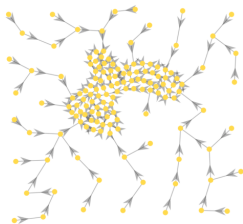
Animation of label propagation with dataset **Compound**

Each peak holds a unique label  
The rest get labels by **ascending** to the peaks

# Label propagation by ascending rule



DP



SD-DP

Animation of label propagation with dataset **Compound**

Each peak holds a unique label  
The rest get labels by **ascending** to the peaks

# Autonomous revision of cluster configuration

Rationale: multi-source **uncertainty**

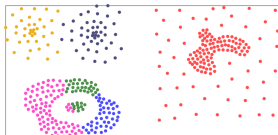
- noise in data
- numerical sensitivity in density calculation
- random tie-breaking in parental node selection

DP

Forward process of peak selection and label propagation without revision



Configuration with 10 clusters

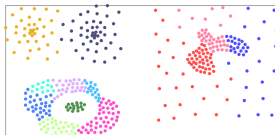


Configuration with #clusters set to 6

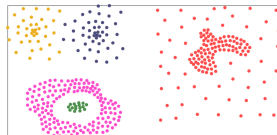
The bottom-left mixture of **Compound** clustered **incorrectly**

SD-DP

Initial configuration of ascending trees at local maxima  
autonomous revision of cluster configuration



Initial configuration



After revision

The bottom-left mixture of **Compound** clustered **correctly**



# Autonomous cluster revision: governing criteria

The weighted  $k$ NN matrix

$$\mathbf{G}_k(i, j) = \underbrace{\mathbf{B}_k(i, j)}_{k\text{NN adjacency}} \exp\left(-\underbrace{(d_{ij} \rho_i^*)}_{\text{relative distance}} / \sigma\right)^2$$

is sparse and encodes density-distance information

**Initial configuration:**  $L$  clusters  $\{\mathcal{C}_p\}$ ,  $1 \leq p \leq L$

$\mathbf{G}_k(\{\mathcal{C}_p\})$  is  $\mathbf{G}_k$  with columns/rows ordered according to the configuration  $\{\mathcal{C}_p\}$

**Optimization Objective:**

$$\{\mathcal{C}_\ell\} = \arg \min_{\{\mathcal{C}_p\}} f(\{\mathcal{C}_p\}), \quad f(\{\mathcal{C}_p\}) = \sum_p |\mathcal{C}_p|^2$$

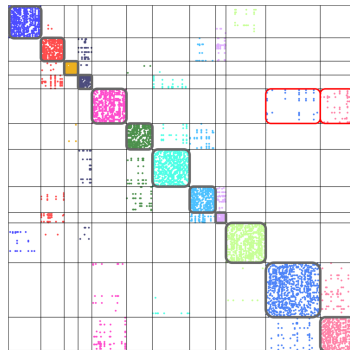
subject to

$$h(\mathbf{G}_k(\mathcal{C}_p, \{\mathcal{C}_q\} - \mathcal{C}_p)) < \tau \cdot h(\mathbf{G}_k(\mathcal{C}_p, \mathcal{C}_p))$$

where

$h(\mathbf{G}_k(\mathcal{C}_p, \mathcal{C}_q))$ : aggregated interaction strength of (sub)matrix

$\tau$ : a small threshold



$\mathbf{G}_k$ :  $k$ NN matrix with rows/columns ordered by initial configuration on **Compound**

Total area of diagonal blocks:  $f(\{\mathcal{C}_p\})$

Aggregated interaction strength:  $h(\mathbf{G}_k(\mathcal{C}_p, \mathcal{C}_q))$

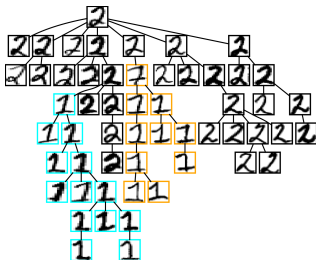
# Autonomous cluster revision: split-and-merge

$\mathbf{G}_k$  is sparse, encodes density-distance information

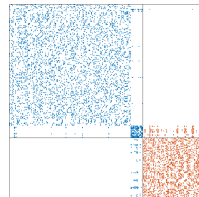
$\mathbf{G}_k(\{\mathcal{C}_p\})$  encodes inter-/intra-cluster interaction strength in addition

A sub-cluster with weak intra-cluster interaction and stronger interaction with another cluster is **split** from its parent and **merged** to the other

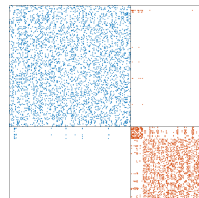
⇒ Inter-cluster interaction strength  $h$  decreases



Subtrees of digit-1 images, initially attached to the parental tree of digit-2 images by local density and the ascending rule, are automatically differentiated from the rest and split from the parental tree



Before split-and-merge



After split-and-merge

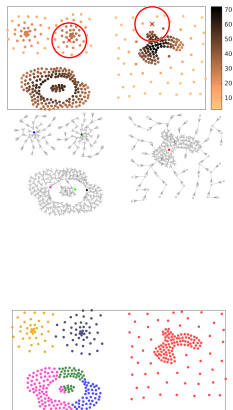
Matrix view of split and merge (synthetic construction)

# Autonomous cluster revision

Animation of autonomous cluster revision with dataset **Compound**

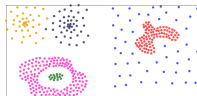
# DP vs SD-DP: clustering process & results

DP



The bottom-left mixture clustered **incorrectly**

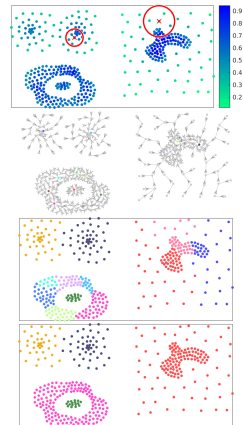
Compound



399 points  
6 classes

The right mixture was not separated;  
it does not adhere to the DP principle

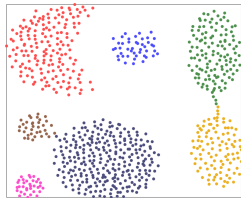
SD-DP



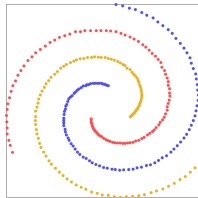
The bottom-left mixture clustered **correctly**

1. Cluster analysis of high-dimensional data
2. The Density Peaks (DP) and other influential algorithms
3. SD-DP: Sparse Dual of the DP algorithm
- 4. Experimental evidence**
  - **Benchmarks**
  - **Exploratory results**

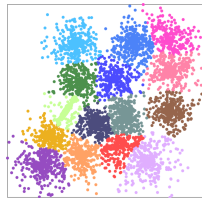
# Benchmark experiments: synthetic benchmarking datasets



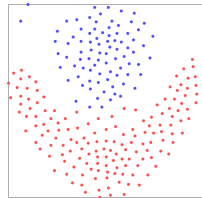
**Aggregation**  
788 points; 7 classes



**Spiral**  
312 points; 3 classes



**S3**  
5,000 points; 15 classes



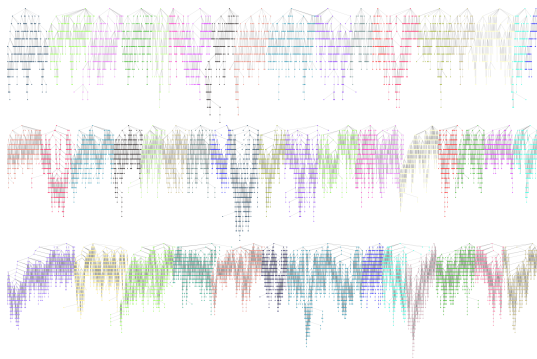
**Flame**  
240 points; 2 classes

SD-DP correctly recovers the numbers and the shapes of the true classes [37]

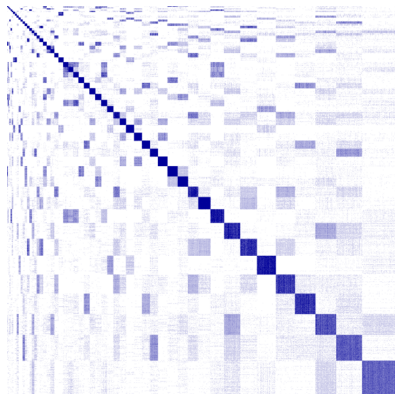
# Benchmark experiments: handwritten digit recognition

Peaks  
(local maxima)

06076711917802698320793166605706137175870032692135984



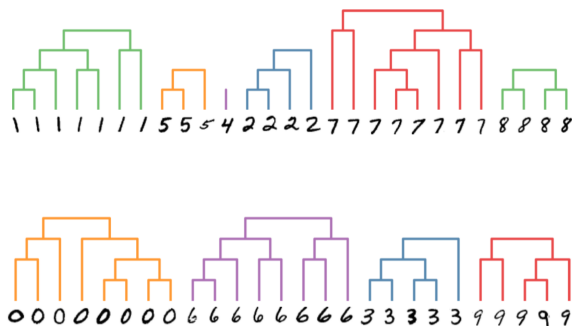
Ascending trees rooted at 53 local maxima; unique color for each tree



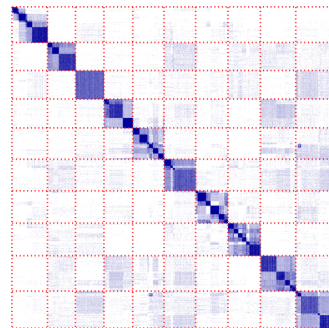
$G_k$ :  $k$ NN matrix with rows/columns ordered by clusters.  
Clusters are arranged in order of size,  $k = 48$

60,000 images of handwritten digits (MNIST dataset)  
HOG descriptor (144 dimensions) for each digit image

# Benchmark experiments: unsupervised revision



Unsupervised cluster merging, unique color for each merged cluster  
Splits took place at a finer level (not shown)



$G_k$ : rows/columns ordered according to two cluster levels – the initial one and the merged one

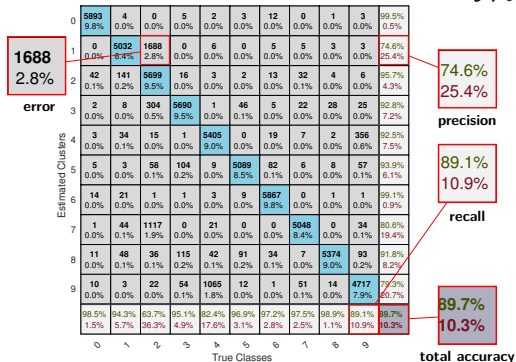


# DP vs SD-DP: classification accuracy

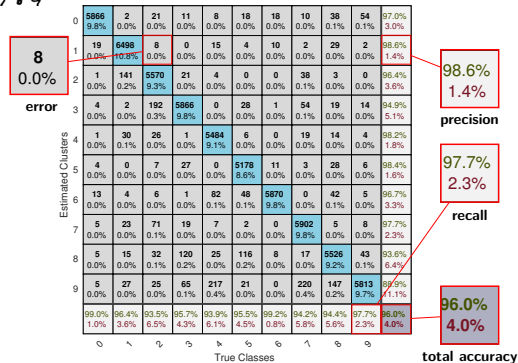
60,000 images of handwritten digits (MNIST dataset) [33]

0 1 2 3 4 5 6 7 8 9  
0 1 2 3 4 5 6 7 8 9  
0 1 2 3 4 5 6 7 8 9  
0 1 2 3 4 5 6 7 8 9  
0 1 2 3 4 5 6 7 8 9

DP (2018) [34]



SD-DP



Intensity feature vector ( $D = 28 \times 28 = 784$ )

Tangent distance

Manual intervention in peak selection and cluster merge

HOG descriptors ( $D = 144$ )

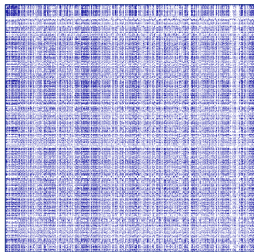
Euclidean distance

Unsupervised cluster revision

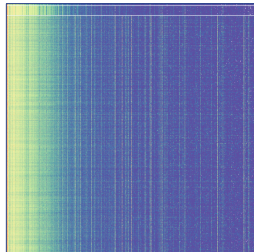
1. Cluster analysis of high-dimensional data
2. The Density Peaks (DP) and other influential algorithms
3. SD-DP: Sparse Dual of the DP algorithm
- 4. Experimental evidence**
  - Benchmarks
  - **Exploratory results**

# DP vs SD-DP: clustering of high-dimensional data

DP



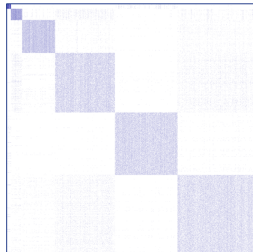
$G_r$ :  $r$ NN matrix with rows/columns ordered by rendered clusters



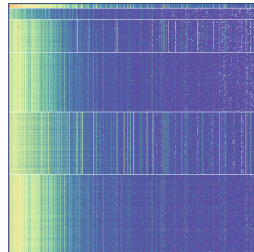
Data matrix cells (rows) vs genes (columns)

DP with  $r = 97.75$  ( $p = 2\%$ )  
Rendered 2 small and 1 large cluster

SD-DP



$G_k$ :  $k$ NN matrix with rows/columns ordered by rendered clusters



Data matrix cells (rows) vs genes (columns)

SD-DP with  $k = 35$   
Rendered 2 small and 4 large clusters

Dataset PBMCs-8k [35]:  $N = 8,000$  cells,  $D = 21,321$  genes

# Exploratory experiments: fast image segmentation



Parthenon image [38] ( $481 \times 321$ ,  $N = 154,401$ )



Segmentation result (3 segments)  
 $5 \times 5$  patch feature per color;  $D = 5 \times 5 \times 3 = 75$

Segmentation time: 3 seconds in MATLAB (excluding  $k$ NN construction)  
SD-DP outpaces DP by two orders of magnitude

# Exploratory experiments: fast high-definition image segmentation



Santorini image<sup>1</sup> ( $1280 \times 800$ ,  $N = 1,024,000$ )



Illustrative segmentation result (30 segments)  
 $9 \times 9$  patch feature per color;  $D = 9 \times 9 \times 3 = 243$

Segmentation time: 15 seconds in MATLAB (excluding  $k$ NN construction)  
SD-DP outpaces DP by at least two orders of magnitude

<sup>1</sup><https://blog.ryanair.com/wp-content/uploads/2015/08/santorini123.jpg>

# Exploratory experiments: statistical hierarchy of word semantics

$N = 400,000$  GloVe [20] word vectors<sup>2</sup> ( $D = 300$ )

Semantically related words, based on word co-occurrence from text content, are closer in the GloVe space

SD-DP ( $k = 5$ ) produces a statistical hierarchy of word semantics

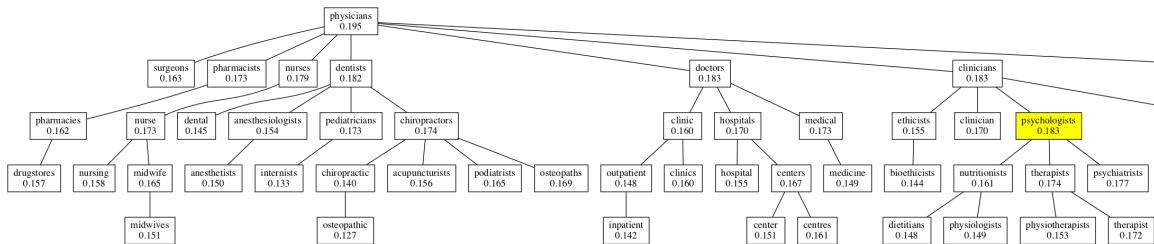
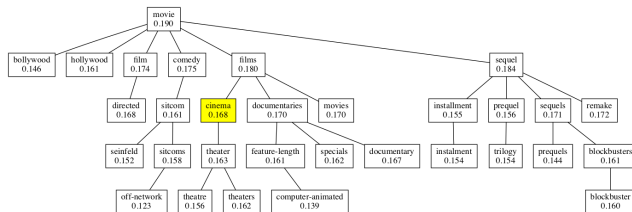
A word with higher density has more general meaning

A word with lower density has more specific meaning

Can be used for search in depth and breadth simultaneously

The local density is annotated on each word

Query words are highlighted



<sup>2</sup>Pre-trained word vectors (Wikipedia 2014 + Gigaword 5)

# Recap: Sparse Dual of Density Peaks

## Contributions

### Dual local density description

ground for robustness, by recognizing, respecting the fundamental facts of high dimensional data

### Initial cluster formation

clusters by ascending trees rooted at local maxima  
proven local, parallel, of linear complexity

### Autonomous cluster revision

coherent revision criteria at multiple cluster levels

### Sparse matrix/graph operations

## Experimental findings

### Unsupervised classification of handwritten digits

96% overall accuracy reached

### Gene clustering

4 large clusters found in 8,000 cells in expression of 21,321 genes

### Statistical hierarchy of word semantics

among 400,000 words in the GloVe space ( $D = 300$ )

### HD image segmentation

faster than DP by two orders of magnitude or more

Algorithms	K-MEANS (1982)	DBSCAN (1996)	OPTICS (1999)	MEAN SHIFT (2002)	GN (2002)	COMBO (2014)	DP (2014)	SD-DP (2018)
Desirable properties								
No prescription of # clusters		✓	✓	✓	✓	✓	✓	✓
No restriction in cluster shape		✓	✓	✓	✓	✓	✓	✓
Free choice of metrics		✓	✓		✓	✓	✓	✓
Agnostic to distribution		✓	✓	✓			✓	✓
Easy or no tuning	✓				✓	✓		✓
Robust in high-dim. space								✓
Accurate in high-dim. space								✓
Low computation cost								✓

# Acknowledgements

Anonymous reviewers for valuable comments

George Bisbas for assistance in experiments

Alexandros-Stavros Iliopoulos for multiple suggestions

Hellenic General Secretariat of Research and Technology and the ERA.NET RUS Plus program for partial support



# References I

- [1] J. Shao, S. W. Tanner, N. Thompson, and T. E. Cheatham, "Clustering molecular dynamics trajectories: 1. Characterizing the performance of different clustering algorithms," *Journal of Chemical Theory and Computation*, vol. 3, no. 6, pp. 2312–2334, 2007.
- [2] I. Zehavi, M. R. Blanton, J. A. Frieman, D. H. Weinberg, H. J. Mo, M. A. Strauss, S. F. Anderson, J. Annis, N. A. Bahcall, M. Bernardi, J. W. Briggs, J. Brinkmann, S. Burles, L. Carey, F. J. Castander, A. J. Connolly, I. Csabai, J. J. Dalcanton, S. Dodelson, M. Doi *et al.*, "Galaxy clustering in early Sloan digital sky survey redshift data," *The Astrophysical Journal*, vol. 571, no. 1, pp. 172–190, 2002.
- [3] M. Girvan and M. E. J. Newman, "Community structure in social and biological networks," *Proceedings of the National Academy of Sciences*, vol. 99, no. 12, pp. 7821–7826, 2002.
- [4] M. E. J. Newman, "Modularity and community structure in networks," *Proceedings of the National Academy of Sciences*, vol. 103, no. 23, pp. 8577–8582, 2006.
- [5] S. Sobolevsky, R. Campari, A. Belyi, and C. Ratti, "General optimization technique for high-quality community detection in complex networks," *Physical Review E*, vol. 90, no. 1, 2014.
- [6] J. Shi and J. Malik, "Normalized cuts and image segmentation," *IEEE Transactions on Pattern Analysis and Machine Intelligence*, vol. 22, no. 8, pp. 888–905, 2000.
- [7] A. Buades, B. Coll, and J.-M. Morel, "A non-local algorithm for image denoising," in *IEEE Conference on Computer Vision and Pattern Recognition*, vol. 2, 2005, pp. 60–65.
- [8] A. W. M. Smeulders, M. Worring, S. Santini, A. Gupta, and R. Jain, "Content-based image retrieval at the end of the early years," *IEEE Transactions on Pattern Analysis & Machine Intelligence*, vol. 22, no. 12, pp. 1349–1380, 2000.
- [9] D. G. Lowe, "Object recognition from local scale-invariant features," in *IEEE International Conference on Computer Vision*, vol. 2, 1999, pp. 1150–1157.
- [10] —, "Local feature view clustering for 3D object recognition," in *IEEE Conference on Computer Vision and Pattern Recognition*, vol. 1, 2001.
- [11] —, "Distinctive image features from scale-invariant keypoints," *International Journal of Computer Vision*, vol. 60, no. 2, pp. 91–110, 2004.

# References II

- [12] N. Dalal and B. Triggs, "Histograms of oriented gradients for human detection," in *IEEE Conference on Computer Vision and Pattern Recognition*, vol. 1, 2005, pp. 886–893.
- [13] A. P. Patel, I. Tirosh, J. J. Trombetta, A. K. Shalek, S. M. Gillespie, H. Wakimoto, D. P. Cahill, B. V. Nahed, W. T. Curry, R. L. Martuza, D. N. Louis, O. Rozenblatt-Rosen, M. L. Suvà, A. Regev, and B. E. Bernstein, "Single-cell RNA-seq highlights intratumoral heterogeneity in primary glioblastoma," *Science*, vol. 344, no. 6190, pp. 1396–1401, 2014.
- [14] A. Zeisel, A. B. Muñoz-Manchado, S. Codeluppi, P. Lönnerberg, G. La Manno, A. Juréus, S. Marques, H. Munguba, L. He, C. Betsholtz, C. Rolny, G. Castelo-Branco, J. Hjerling-Leffler, and S. Linnarsson, "Cell types in the mouse cortex and hippocampus revealed by single-cell RNA-seq," *Science*, vol. 347, no. 6226, pp. 1138–1142, 2015.
- [15] D. Grün, A. Lyubimova, L. Kester, K. Wiebrands, O. Basak, N. Sasaki, H. Clevers, and A. van Oudenaarden, "Single-cell messenger RNA sequencing reveals rare intestinal cell types," *Nature*, vol. 525, pp. 251–255, 2015.
- [16] A. M. Klein, L. Mazutis, I. Akartuna, N. Tallapragada, A. Veres, V. Li, L. Peshkin, D. A. Weitz, and M. W. Kirschner, "Droplet barcoding for single cell transcriptomics applied to embryonic stem cells," *Cell*, vol. 161, no. 5, pp. 1187–1201, 2015.
- [17] J. M. Lee and E. L. Sonnhammer, "Genomic gene clustering analysis of pathways in eukaryotes," *Genome Research*, vol. 13, no. 5, pp. 875–882, 2003.
- [18] I. S. Dhillon, "Co-clustering documents and words using bipartite spectral graph partitioning," in *Proceedings of 7th International Conference on Knowledge Discovery and Data Mining*, 2001, pp. 269–274.
- [19] W. Xu, X. Liu, and Y. Gong, "Document clustering based on non-negative matrix factorization," in *Proceedings of the 26th Annual International ACM SIGIR Conference on Research and Development in Informaion Retrieval*, 2003, pp. 267–273.
- [20] J. Pennington, R. Socher, and C. D. Manning, "GloVe: Global vectors for word representation," in *Empirical Methods in Natural Language Processing*, 2014, pp. 1532–1543.
- [21] N. Scaringella, G. Zoia, and D. Mlynek, "Automatic genre classification of music content: a survey," *IEEE Signal Processing Magazine*, vol. 23, no. 2, pp. 133–141, 2006.

# References III

- [22] A. Shepitsen, J. Gemmell, B. Mobasher, and R. Burke, "Personalized recommendation in social tagging systems using hierarchical clustering," in *Proceedings of the 2008 ACM Conference on Recommender Systems*, 2008, pp. 259–266.
- [23] ESO, "An intergalactic heavyweight," 2013, <https://www.eso.org/public/images/potw1304a/>.
- [24] G. Bisbas, "Forecast demand using extended discrete Fourier transform. (in Greek)," Diploma thesis, Aristotle University of Thessaloniki, Greece, 2017.
- [25] K. Mylonakis, N. Pitsianis, and X. Sun, "The fast multipole method in three decades," Poster presented at Epstein Greengard Modern Advances in Computational and Applied Mathematics workshop at Yale University, 2017.
- [26] NASA, "City Lights of the United States," 2012, <https://earthobservatory.nasa.gov/images/79800/city-lights-of-the-united-states-2012>.
- [27] S. P. Lloyd, "Least squares quantization in PCM," *IEEE Transactions on Information Theory*, vol. 28, no. 2, pp. 129–137, 1982.
- [28] M. Ester, H.-P. Kriegel, J. Sander, and X. Xu, "A density-based algorithm for discovering clusters in large spatial databases with noise," in *Proceedings of 2nd International Conference on Knowledge Discovery and Data Mining*, 1996, pp. 226–231.
- [29] M. Ankerst, M. M. Breunig, H.-P. Kriegel, and J. Sander, "OPTICS: ordering points to identify the clustering structure," *ACM Sigmod Record*, vol. 28, no. 2, pp. 49–60, 1999.
- [30] D. Comaniciu and P. Meer, "Mean shift: a robust approach toward feature space analysis," *IEEE Transactions on Pattern Analysis and Machine Intelligence*, vol. 24, no. 5, pp. 603–619, 2002.
- [31] A. Rodriguez and A. Laio, "Clustering by fast search and find of density peaks," *Science*, vol. 344, no. 6191, pp. 1492–1496, 2014.
- [32] D. Floros, T. Liu, N. Pitsianis, and X. Sun, "Sparse dual of the density peaks algorithm for cluster analysis of high-dimensional data," in *IEEE High Performance Extreme Computing Conference*, 2018.
- [33] Y. Lecun, L. Bottou, Y. Bengio, and P. Haffner, "Gradient-based learning applied to document recognition," *Proceedings of the IEEE*, vol. 86, no. 11, pp. 2278–2324, 1998.

# References IV

- [34] M. d'Errico, E. Facco, A. Laio, and A. Rodriguez, "Automatic topography of high-dimensional data sets by non-parametric Density Peak clustering," 2018, arXiv:1802.10549.
- [35] G. X. Zheng, J. M. Terry, P. Belgrader, P. Ryvkin, Z. W. Bent, R. Wilson, S. B. Ziraldo, T. D. Wheeler, G. P. McDermott, J. Zhu *et al.*, "Massively parallel digital transcriptional profiling of single cells," *Nature Communications*, vol. 8, 2017.
- [36] C. T. Zahn, "Graph-theoretical methods for detecting and describing gestalt clusters," *IEEE Transactions on Computers*, vol. C-20, no. 1, pp. 68–86, 1971.
- [37] P. Fränti and S. Sieranoja, "K-means properties on six clustering benchmark datasets," *Applied Intelligence*, vol. 48, 2018, <http://cs.uef.fi/sipu/datasets/>.
- [38] D. Martin, C. Fowlkes, D. Tal, and J. Malik, "A database of human segmented natural images and its application to evaluating segmentation algorithms and measuring ecological statistics," in *IEEE International Conference on Computer Vision*, vol. 2, 2001, pp. 416–423.